Low Temperature Physics/Fizika Nizkikh Temperatur, 2013, v. 39, No. 10, pp. 1146–1155

Aging of solid ^{4}He under torsional oscillation at low temperatures

P. Gumann* and H. Kojima

Serin Physics Laboratory, Rutgers University, Piscataway, NJ 08854, USA
E-mail: kojima@physics.rutgers.edu

Received March 12, 2013

Observations have been made to reveal unusual aging behavior in solid ^{4}He samples contained in a torsional oscillator. Oscillation of samples is initiated at a given oscillator drive amplitude near 100 mK. After the samples are cooled to a measurement temperature, they are "aged" for a waiting time, t_w, between 15 min and 25 h. The drive amplitude is then halved and subsequent variation in the oscillator response amplitude, $A(t)$, and frequency are monitored as time t elapses. When the measurement temperature is lower than T_s = 40 mK, $A(t)$ shows unusual behavior: $A(t)$ initially undershoots to less than half of the original value, partially recovers exponentially and eventually continues to increase logarithmically. The amount of undershoot, partial recovery magnitude and the rate of logarithmic increase all show aging effect with logarithmic dependence on t_w. When the measurement temperature is greater than T_s, the above unusual behavior in $A(t)$ disappears. If solid ^{4}He cooled below T_s behaved analogously to spin glasses, $A(t/t_w)$ would be independent of t_w. Such behavior of $A(t/t_w)$ is not observed. Origin of the unusual aging behavior in solid ^{4}He is not yet clear. Motion of dislocation lines is discussed as a possible origin.

PACS: **67.80.–s** Quantum solids;
67.80.dj Defects, impurities, and diffusion;
64.70.–p Specific phase transitions;
62.20.Hg Creep;
62.40.+I Anelasticity, internal friction, stress relaxation, and mechanical resonances.

Keywords: quantum solid, supersolid, aging, glass, dislocation, creep.

1. Introduction and motivation

Observations [1,2] that hcp solid ^{4}He appeared to partially decouple from its torsionally oscillating container at temperatures below 300 mK led to the interpretation as the long-sought superfluidity in solid ^{4}He or supersolidity. Though the apparent decoupling effect as evidenced by the drop in the period of torsional oscillator (TO) has been reproduced in many laboratories [3,4], the supersolidity interpretation has been met with considerable skepticism. Day and Beamish [5] discovered that the shear modulus of solid ^{4}He showed strikingly similar behaviors as those found in torsional oscillator experiments in temperature dependence, nonlinearity and hysteresis [6] in drive dependence, and dependence on ^{3}He impurity [7–9]. These similarities pointed to the shear modulus of solid ^{4}He contributing, at least in part, to the observed decoupling effects in TO experiments. Recently reported TO experiments showed that the decoupling effect disappeared [10] when the small sample space between the Vycor substrate and the container wall was eliminated. This report has apparently ruled out supersolidity as the explanation of the decoupling of solid ^{4}He in Vycor. A full explanation of the period drop in other TO experiments, however, still needs to be established.

Roles of glassy disorder [11–15] such as in dislocation lines [16] and grain boundaries [17] in the observed decoupling effect in solid ^{4}He have been explored theoretically. Interpreting disordered solid ^{4}He in terms of a two-level system [18–22] would predict glassy behavior of solid ^{4}He. Dramatic changes in decoupling effects in TO were observed [23] between pre-annealed and post-annealed solid ^{4}He sample. The annealing effect clearly demonstrated the importance of disorder in samples. Hints of glassy disorder were found by Aoki *et al.* [24]

* Present address: Institute for Quantum Computing, University of Waterloo, Waterloo, ON, Canada

who observed long and unusual relaxation in their "field-cooled" (see below) experiments. Hunt *et al.* [25,26] made systematic measurements of relaxation and analyzed their data in terms of a glassy behavior.

A signature indicating glassy state is a linear temperature dependence of heat capacity. The small heat capacity of solid ^{4}He has made it difficult [27,28] to discern a presence of linear temperature dependence. Anomalies [29] in the temperature dependence of heat capacity of solid ^{4}He around the temperature where TO period drop occurred have been reported. Associated with the linear temperature dependence of heat capacity is a quadratic temperature dependence of pressure. Experiments by Grigore'v *et al.* [30] indeed showed that the pressure of non-annealed solid ^{4}He samples varied quadratically with temperature below 300 mK.

A clear finger print of glassy materials is their age dependent behavior. Aging is observed [31–33] in spin glasses, for example, by cooling them under an external dc magnetic field to a measurement temperature, T_m, below their glass transition temperatures and waiting for time interval t_w during which aging occurs. The field is then removed and the subsequent time, t, dependence of the magnetization or the ac magnetic susceptibility $\chi(t)$ of the materials are monitored as the system relaxes. The observed nonexponential time dependent relaxation is found to depend on both t_w and t. The time dependent magnetization relaxation has inflection points (peaks in the quantity $\partial\chi/\partial(\ln t)$) which increase as t_w is increased. Furthermore, the measured magnetization plotted against t/t_w is independent of t_w.

Numerical studies [34] have shown that the dynamics of dislocations exhibit various glassy behavior including aging similar to those found in spin glasses. The motivation for the present work is to search for such age dependent behavior in disordered solid ^{4}He having dislocation lines at low temperatures. The present report describes our measurements designed to look for aging behavior in annular solid ^{4}He samples contained in a TO. The samples are field-cooled from a "high" temperature (~ 100 mK) while holding the TO drive level constant to a measurement temperature T_m. After waiting a time interval t_w, the drive amplitude is decreased to half. The relaxation of the measured TO oscillation amplitude $A(t)$ following the decrease in drive amplitude is monitored up to 24 h.

2. Apparatus and procedure

The TO in the experiments described here is a double compound oscillator which allows studies of mechanical response at two distinct oscillation frequencies. Operation of double compound oscillator has been described previously [6,35]. The sample container attached to the TO is a thin annulus (10.0 mm outer diameter, 9.6 inner diameter, 8.0 mm height). The cell design is essentially identical to that described in detail by Gumann *et al.* [9] except for the thickness of the annular sample chamber. The sample chamber is filled through a hole (0.8 mm diameter) drilled into the BeCu torsion rod (2.0 mm diameter) of the TO. The TO is attached to a vibration isolation block which is in turn attached to the mixing chamber of a dilution refrigerator.

It has been pointed [36] out that the observed TO frequency shifts in our first double compound oscillator might be dominated by changes in the shear modulus of ^{4}He within the torsion rod and that the frequency shifts might not be related to the solid in the sample chamber itself. In the Appendix section, this ambiguity is critically examined and it is concluded that the observed frequency shifts in our TOs arise from the effects of solid ^{4}He in the sample chamber.

The background resonant frequencies of the TO at 250 mK with the sample chamber empty are f_{1b} = 465 Hz and f_{2b} = 1091 Hz with quality factors of $4\cdot10^5$ and $3\cdot10^5$ for the first and second mode, respectively. Prior to loading the sample chamber with solid ^{4}He, the background temperature, T, dependence of the frequency and amplitude of both modes are measured. The "background" measurement is also taken at the end of measurements with the sample chamber filled with superfluid at 17 bar. The temperature dependence of the two background measurements are consistent with each other. This demonstrates that the internal stress exerted to the TO by the sample pressure does not alter its mechanical properties.

Solid ^{4}He samples are grown by the blocked capillary method and are likely highly disordered. Briefly, the sample chamber is first filled with liquid by condensing ^{4}He gas (nominal high purity with 0.3 ppm ^{3}He concentration) at 4.2 K at a given loading pressure. Rapidly cooling the upper segment of the fill tube freezes the liquid contained there and produces a solid block. Subsequently the helium below the block is cooled at constant mass. The helium in the sample chamber is solidified within the next one hour or so by cooling via the mixing chamber. The changes in resonant frequency due to loading the sample chamber at 78 bar (creating a solid sample at ~ 35 bar) are Δf_1 = = 173 mHz and Δf_2 = 313 mHz for the first and second mode, respectively, in agreement within 10 % with estimates based on cell dimensions and materials.

Measured temperature dependence of the resonant frequencies, $f_1(T)$ and $f_2(T)$ of the sample-loaded TO is different from that of the background of the empty TO. The difference has been termed [1,37] nonclassical rotational inertia fraction (NCRIf). Choosing, somewhat arbitrarily, a reference temperature T_0 = 250 mK, temperature and mode (i = 1, 2) dependent NCRIf$_i$ is defined as $\delta f_i(T)/\Delta f_i$, where $\delta f_i(T) = [f_i(T) - f_i(T_0)] - [f_{ib}(T) - f_{ib}(T_0)]$. The maximum low-temperature values of NCRIf$_i$ in the present annular sample chamber are found to be 0.7 and 2.6 % for i = 1 and 2, respectively. These NCRIf$_i$ are much larger than those found earlier [6] in a cylindrical sample chamber. Further-

more, $NCRIf_2 \gg NCRIf_1$ in contrast to the mode-independent NCRIf in cylindrical [6] sample chamber. Characteristic peaks in dissipation are also observed for each mode in the temperature range where $NCRIf_i$ changes rapidly. This report focuses not on the TO frequencies but on the response amplitude that exhibits clearer aging effects.

The two resonant modes of the double compound TO can be driven simultaneously by applying a summed voltage, $V = V_0 + V_{1ac}\sin(2\pi f_1 t) + V_{2ac}\sin(2\pi f_2 t)$, between the moving "fin" electrode attached to the TO and a fixed electrode, where V_0 is a dc bias and V_{iac} is the ac drive amplitude for the mode i. The drive frequencies f_i may be continually tracked at resonance by automatically maintaining constant phases between the drive and signal of each mode using two independent lock-in amplifiers. The TO oscillation response amplitude A_i is also continuously monitored. In the standard protocol (see below) of the measurements reported here, the focus is on the mode 2. The mode 1 is driven at a very low constant drive amplitude only for the purpose of monitoring the sample temperature. The low drive amplitude of the mode 1 does not affect the observed aging effects of the mode 2 in any significant manner.

Our standard protocol to search for aging effects in torsionally oscillated solid ^{4}He is as follows. The sample in the TO is "velocity-field cooled" starting from about 100 mK down to a measurement temperature T_m over approximately one hour while driving the mode 2 with V_{2ac} = 100 mV (this drive produces a velocity amplitude of 255 μm/s at the outer rim of the sample). Though systematic study was not carried out, results do not depend significantly on the time taken for cooling up to three hours. After waiting a time interval of t_w at T_m, V_{2ac} is decreased to 50 mV over about 480 s which is long enough to avoid initiating ringing. Ensuing time dependent $A_2(t)$ and $f_2(t)$ are measured continuously for up to 24 h. At the end of measurement for a given t_w, the drive amplitude is increased back up to 100 mV and the process is repeated by warming up to 100 mK (except as noted below) where "memory" of the sample history is erased. The system is cooled down again to T_m to repeat measurement with a different t_w. The standard protocol is repeated at T_m equal 10, 20, 32, 40, 50, 80, and 100 mK. In the measurement at T_m = 100 mK, the sample temperature is warmed up to 200 mK to erase the sample history. When this process is carried out with the sample space filled with superfluid at 17 bar, $A_i(t)$ is independent of t_w and there are no aging effects described below.

3. Results

An example of data taken with the standard protocol is shown in Fig. 1 displaying the second mode signal amplitude as a function of time. Notation is simplified by defining $A_2 \equiv A$. The drive amplitude V_{2ac} is decreased from 100 to 50 mV and increased back up to 100 mV at the times shown in Fig. 1. The response just after the decrease

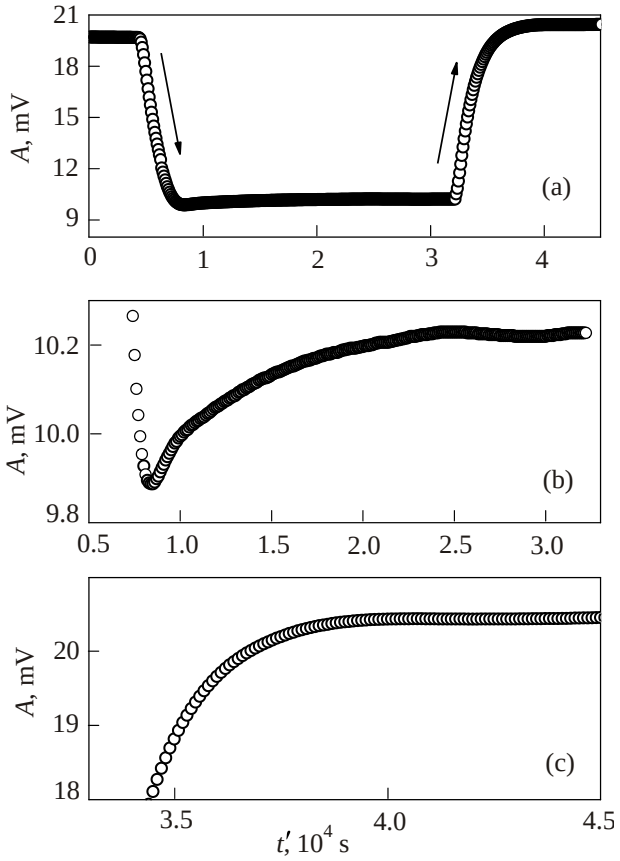

Fig. 1. Example of response amplitude of the mode 2 taken at T_m = 32 mK and $t_w = 1.02\cdot10^4$ s. Elapsed time t' starts at an arbitrary initial time. Panel (a) includes time response during and after decrease (indicated by downward arrow) in drive amplitude from 100 mV to 50 mV at $t' = 0.44\cdot10^4$ s and increase (indicated by upward arrow) in drive amplitude back to 100 mV at $t' = 3.22\cdot10^4$ s. Panel (b) shows an expanded view after the decrease. Panel (c) shows an expanded view after the increase in drive amplitude.

in drive amplitude is expanded in panel Fig. 1(b) which shows initial "undershoot" and a subsequent *nonexponential* recovery in the signal amplitude. Observed time dependent behavior during the undershoot and recovery depends on both t_w and T_m and is analyzed below in detail. The signal amplitude displayed in Fig. 1 (c) after the increase in drive amplitude back up to the original value shows an exponential approach to a final amplitude. An overshoot upon the increase in drive amplitude might be expected in analogy to the undershoot upon the reduction in drive amplitude, but that is not observed. It should be noted that the final response amplitude is greater than the initial amplitude before the decrease in drive amplitude. Clearly, the state of the sample after reducing the drive amplitude is quite different from the initial state with the original drive amplitude. Studies on this hysteresis phenomenon were reported [38] previously.

The oscillator frequency also shows relaxation during the time span shown in Fig. 1. Since there is more scatter in the frequency data and the development of aging as t_w is varied is not so clear, we focus only on the response amplitude data.

Dependence on the final drive amplitude in the aging experiment protocol is studied [39] by keeping the initial drive amplitude constant but varying the final drive amplitude between 90 to 5 % of the initial value. Although the amount of undershoot increases as the final drive amplitude is decreased, the qualitative behavior of the subsequent relaxation is similar. In all of the experiments reported here, the final drive amplitude is kept constant at half of the initial drive amplitude.

Let A_0 be the signal amplitude after waiting for t_w at the temperature T_m with the drive amplitude of 100 mV. There is a small but systematic increase in A_0 as t_w is increased as shown in the inset to Fig. 2. Thermal equilibration time is less than 10^3 s and the observed increase is likely not related to the sample temperature equilibration process.

Time dependence of the "reduced" response amplitude $A(t)/A_0$ is displayed in Fig. 2 as t_w is varied. The time t is defined as the elapsed time from the time t' when the signal amplitude reaches the minimum (located within ±10 s) for the data with a given t_w.

The "initial" reduced amplitude $r_i \equiv A(t_i)/A_0$ at t_i = = 10 s and the "final" reduced amplitude $r_f \equiv A(t_f)/A_0$ (extrapolated in some cases) at $t_f = 4\cdot10^3$ s both for the data in Fig. 2 are shown in Fig. 3. Clearly r_i (r_f) increases (decreases) significantly as t_w is increased or as the sample is aged. Figure 3 indicates that the initial (final) amplitude increases (decreases) logarithmically with t_w. Even after our largest t_w of 24 h, both r_i and r_f continue to change. Similar measurements as in Fig. 2 at other T_m

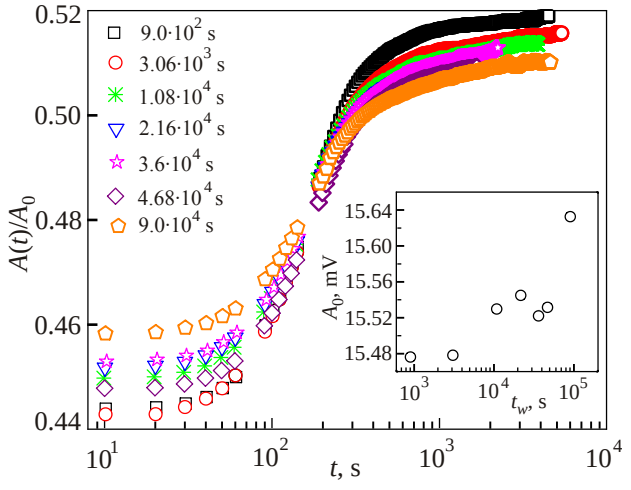

Fig. 2. (Color online) Time dependence of reduced response amplitude after various waiting times at 32 mK. Waiting times t_w are 15 min (□), 51 min (○), 3 h (✳), 6 h (▽), 10 h (◇), 13 h (☆), 25 h (⬡). The gaps in data around $A(t)/A_0$ ~ 0.48 are electronics-related and not significant.

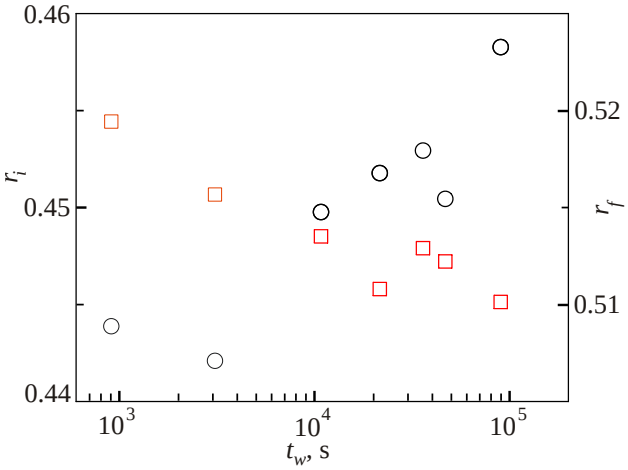

Fig. 3. (Color online) Initial and final reduced amplitudes (see text). The plotted values are taken from Fig. 2. Both the initial (left ordinate, ○) and final (right ordinate, □) amplitudes have not reached stable values after aging for t_w = 24 h.

reveal that the initial reduced amplitude decreases sharply over a narrow temperature range near 40 mK (see below).

All plots in Fig. 2 *almost* collapse onto each other when the reduced amplitude is renormalized by taking the ratio $(A(t)/A_0 - r_i)/(r_f - r_i)$ as shown in Fig. 4. Displaying the data in this manner shows that there is little, if any, aging dependence in the time dependence of renormalized response amplitude at 32 mK. See below for more precise analysis using a specific time dependent fitting function.

Temperature dependence of the reduce response amplitude is displayed in Fig. 5. Figure 5(a) shows that there is strong dependence of $A(t)/A_0$ on T_m. The initial reduced amplitude r_i read off panel (a) is plotted in panel (b). Figure 5(b) shows that r_i decreases rapidly above 20 mK but increases above 50 mK.

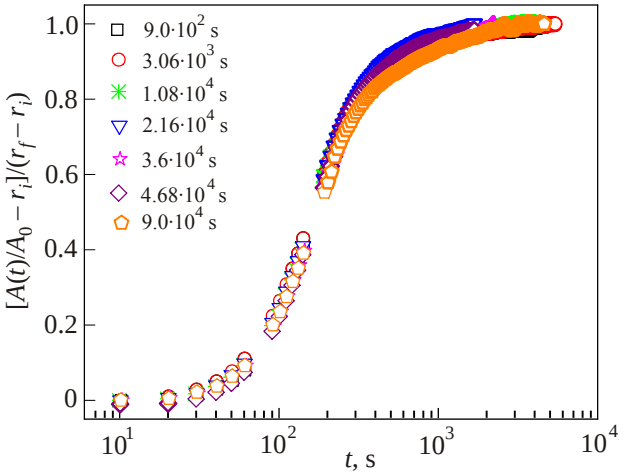

Fig. 4. (Color online) Renormalized (see text) response amplitude of the data shown in Fig. 2. All data collapse onto each other regardless of waiting time. Symbols correspond to the same waiting times as shown in Fig. 2.

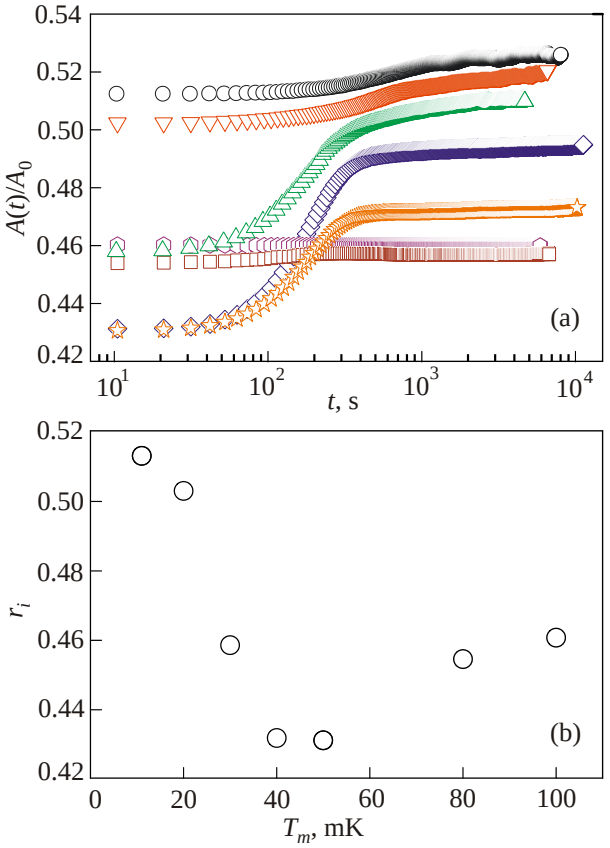

Fig. 5. (Color online) Fractional amplitude $A(t)/A_0$. Panel (a): measured at T_m (in mK), (t_w (in hours), symbols) = 11 (11.25, ○), 20 (24, ▽), 32 (25, △), 40 (23, ◇), 50 (22.25, ☆), 80 (18.5, □), and 100 (16, ⬡). Panel (b): initial reduced amplitude read from panel (a) at t = 10 s.

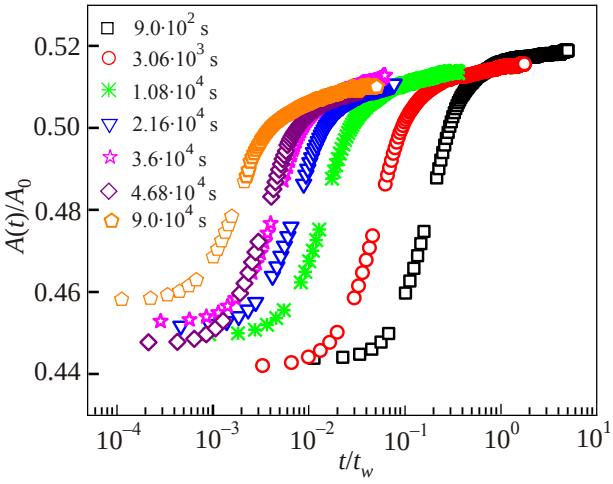

Fig. 6. (Color online) Reduced response amplitude shown in Fig. 2 plotted against reduced time. If similar aging time dependence as the magnetization of spin glass materials [41] were present, the plot would overlap (see text). Symbols correspond to the same waiting times as shown in Fig. 2.

What happens when the sample is cooled in zero velocity field (zero drive amplitude), wait t_w, turn on the field and then measure $A(t)$? This procedure would examine dependence of the aging process on the applied drive amplitude. This is an interesting question, but the experiment would be difficult to carry out owing to long ringing time effects. Annealing the sample by warming it to above1 K is expected to alter the aging process but such annealing studies have not been carried out.

To be sure that the observed time dependece as shown in Fig. 1 occurs in the presence of solid ^{4}He in the sample chamber, the same measurement protocol was followed with the sample chamber filled with superfluid ^{4}He. In this case, there is only a ring down effect as the drive amplitude is decreased. Clearly, it is the presence of solid ^{4}He sample that produces the undershoot and subsequent recovery over long time interval.

4. Analysis

Before proceeding with detailed analysis, let us recall an analogous aging experiment carried out on spin glasses. In a so-called "thermo-remanent magnetization" measurement [40,41], a spin glass sample is cooled under a magnetic field H in a short time interval and the field is switched off after waiting a time interval t_w and the magnetization $M(t)$ is subsequently measured as time t (= 0 when the field is switched off) elapses. Measurements show that $M(t)$ has inflection points at times $t \approx t_w$ [40]. Aging portions of $M(t)$ plotted against "reduced time" t/t_w lie on top of each other [41]. This universal behavior of $M(t)$ on t/t_w and the time of inflection increasing as t_w is increased are taken as characteristic signatures of "simple" aging in glassy materials.

The measured response amplitude $A(t)$ in our TO experiment may be considered as the inverse of the imaginary (dissipative) part of the complex rotational susceptibility of solid ^{4}He contained in the sample chamber. If rotationally oscillated solid ^{4}He behaved as a glass, $A(t)/A_0$ might exhibit qualitatively similar aging behavior as magnetization of spin glass materials. The data shown in Fig. 2 are replotted against the reduced time t/t_w in Fig. 6. Clearly plots of $A(t/t_w)/A_0$ for different values of t_w do not overlap. This is in stark contrast to the universality [41] of $M(t/t_w)$ of spin glasses.

Time derivatives of the reduced response amplitude, $d[A(t)/A_0]/dt$, are shown in Fig. 7. There is a pronounced peak in the derivative, or an inflection point, for each t_w data. The inflection point all occurs at $t \sim$ 120 s independently of t_w unlike the inflection points in $M(t)$ of spin glasses which vary in proportion to t_w.

Thus, the aging effects of universal dependence on t/t_w and dependence of inflection point on t_w seen in thermo-remanent magnetization measurements of spin glasses are not present in the response amplitude of TO containing solid ^{4}He. There are, however, aging dependent characteristics

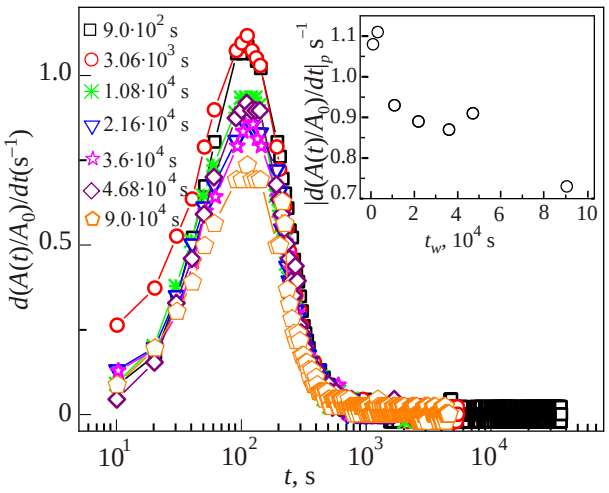

Fig. 7. (Color online) Time dependence of time rate of change of amplitude at 32 mK. Symbols correspond to the same waiting times as shown in Fig. 2. Inflection point occurs at t = 120 s common to all data with different waiting time t_w. Lines merely connect data points. If similar aging time dependence as the magnetization of spin glass materials [40] were present, the time at inflection point would increase as t_w is increased (see text). Inset: magnitude of time derivative of A at inflection points.

such as the response amplitude A_0 before the drive amplitude is decreased (see inset to Fig. 2), the initial response amplitude r_i just after the drive is decreased and the "final" response amplitude in the long time limit (see Fig. 3). A time dependent function for fitting $A(t)/A_0$ is developed next to explore possible aging dependence in the fitting parameters that enter.

Inspection of the time dependence of $A(t)/A_0$ shown in Fig. 2 suggests three processes are involved. One is the ring down that occurs when the drive amplitude applied to a high Q oscillator resonance is reduced. Another is a recovery process from the undershoot that occurs at the end of the ring down. Finally, a slow creep process that continues at all times. It is found that $A(t)/A_0$ can be fitted well by a sum of functions describing exponential ring down following the decrease in drive level, subsequent exponential recovery and finally slow logarithmic creep:

$$A(t)/A_0 = r_i + a[-1+e^{-t/\tau_r}] + b[1-e^{-t/\tau_0}] + c[\log t] \quad (1)$$

where a, b, c, τ_r, τ_0 are fitting parameters. The value of r_i is set by $A(t_i)/A_0$ in Fig. 3. As defined above, the time t is set to zero when the signal amplitude reaches the minimum. The initial ring down is described by the terms in the first square bracket in Eq. (1) with amplitude a and ring down time τ_r. The recovery part is described by the terms in the second square bracket in Eq. (1) with fitting parameters, b and τ_0. Finally, the slow variation after the recovery is described by a logarithmic time dependence with the fitting parameter c. Stretched exponential functions were attempted but satisfactory fit could not be achieved for the time dependence of the recovery and slow long time tail.

An example of fit to $A(t)/A_0$ using Eq. (1) is shown in Fig. 8. Equally excellent fits are obtained at other values of t_w and at other temperatures. Dependence of the fitting parameters on t_w at 32 mK is shown in Fig. 9. There is considerable scatter in many of the fitting parameters. The ring-down parameter a is independent of aging within the scatter. The ring-down time τ_r tends to increase as aging is increased (except for the outlier at t_w = 25 h). The recovery parameter b shows a slight tendency to decrease as aging is increased. The recovery relaxation time τ_0 decreases as aging is increased (except again for the outlier at t_w = 25 h). Unfortunately, the large scatter in the most interesting logarithmic dependence does not allow making a definitive aging dependence of the parameter c. However, panel (c) in Fig. 9 appears to indicate an increasing trend in c as t_w is increased. This is surprising since aging is expected to "slow down" the process towards equilibrium.

Temperature dependence of the best-fit values of a, b, c, τ_r, and τ_0 for the data displayed in Fig. 5 are shown in Fig. 10. The parameters a, b and τ_r decrease, within their respective scatters, as T_m is increased. On the other hand, c and τ_0 show markedly different behavior in low- and high-temperature ranges separated by an onset temperature for a slowing down or creeping process, T_s, near 40 mK. Both of these parameters nearly vanish when $T_m > T_s$ but become much greater when $T_m < T_s$.

We have studied hysteresis [6,38] loops in both the frequency and amplitude of TOs loaded with solid ^{4}He samples when the drive amplitude is varied. It has been shown [38] that the hysteresis occurs only below an onset temperature T_H which depends on the dimensions and possibly on the geometry of the sample chamber and ^{3}He impurity concentration. It is interesting to ask how this T_H and the

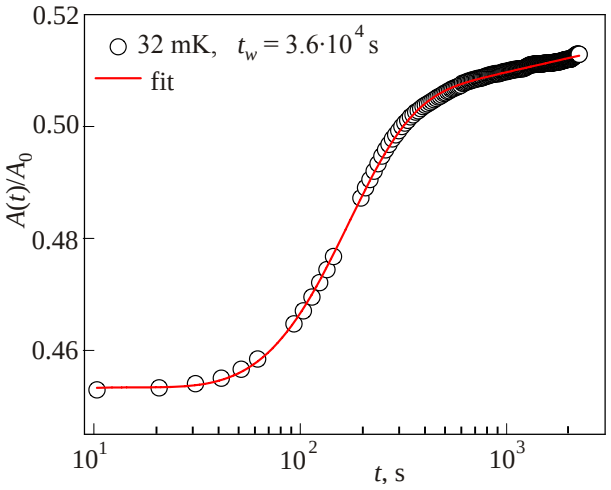

Fig. 8. (Color online) Fitting $A(t)/A_0$ data at 32 mK and $t_w = 3.6\cdot10^4$ s with Eq. (1) which accounts for ring down, recovery and logarithmic time dependence (see text). The fitting parameter values here are: a = 1.147, b = 1.801, c = 0.090, τ_r = 59 s, and τ_0 = 95 s.

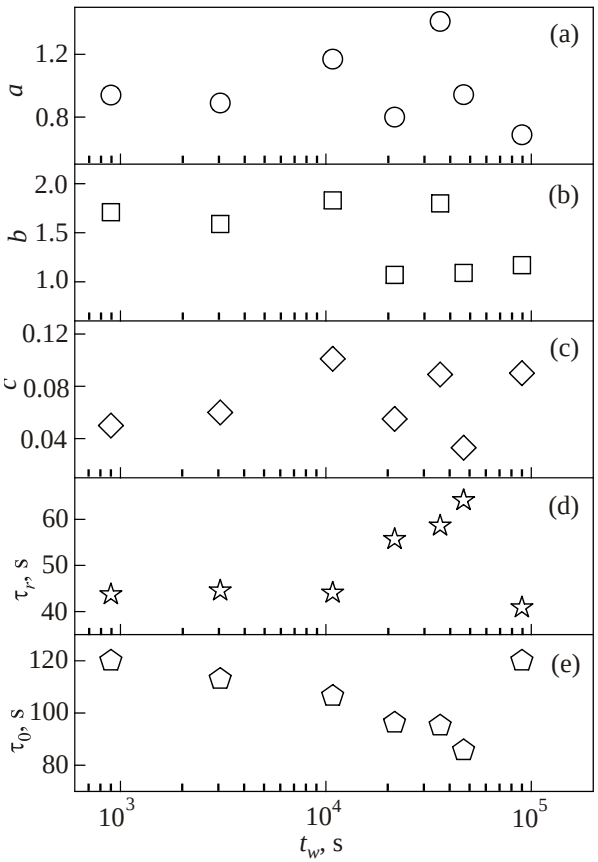

Fig. 9. Adjusted parameters at 32 mK. Best fit parameters in Eq. (1) are plotted for the data in Fig. 2 as t_w is varied. Variations of the parameters are smooth up to about ~ 20 h but show sudden change in the data for t_w = 24 h.

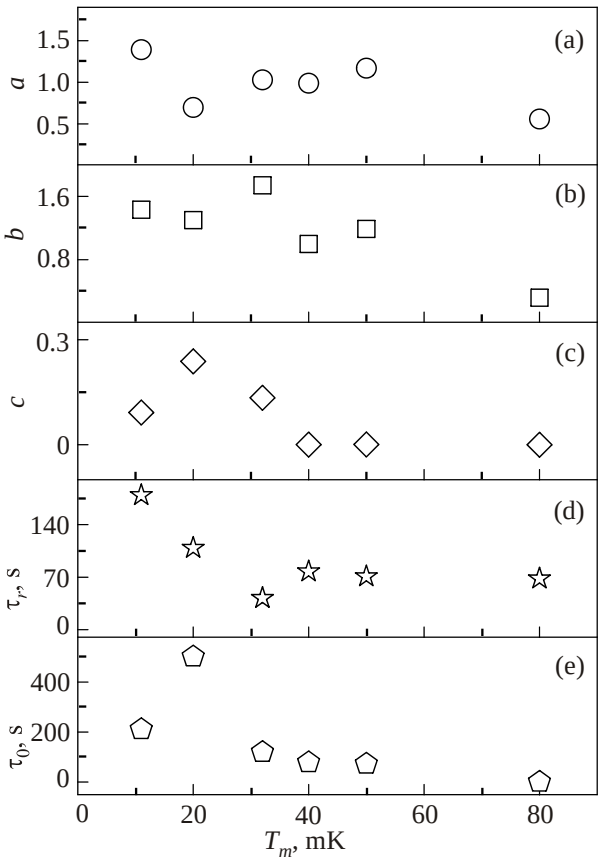

Fig. 10. Temperature dependence of best fit parameters in Eq. (1) to those data shown in Fig. 5. The logarithmic dependence (see parameter *c*) is seen to disappear at T $\gtrsim$ 40 mK.

new onset temperature T_s might be related to each other. In the identical TO with the same annular sample chamber and the same nominal ^{3}He concentration, T_H was measured [38] to be 70 mK. Allowing for possible ± 10 mK error in determination of T_H and T_s, these characteristic temperatures appear to be distinct. As the solid ^{4}He temperature is decreased, hysteresis sets in first and then a long logarithmic creep sets in at a lower temperature. The hysteresis and the creep phenomena apparently have different physical mechanisms.

5. Discussion

In our earlier experiment [6] with cylindrical (10.2 mm diameter and 7.6 mm height) sample chamber, the unusual time dependent behavior of undershoot, subsequent recovery and long time logarithmic decay was discovered in the similar experimental protocol as the present one. The observed total change in TO response amplitude from the minimum at the undershoot to the maximum seen during logarithmic decay is ten times larger at 32 mK in the present 0.2 mm wide annular sample chamber than in the previous cylindrical sample chamber. Temperature dependence was studied in the cylindrical sample chamber but not aging effects on waiting time t_w. Time dependence of TO response amplitude could be fitted with a similar form as Eq. (1). The relaxation time τ_0 characterizing the recovery increased rapidly below about 30 mK in the cylindrical sample (see Fig. 4 of Aoki *et al*. [24]). In the present 0.2 mm wide annular sample, τ_0 increases below about 40 mK (see Fig. 10) but its temperature dependence is not well established. The fitting parameter *b* showed nonmonotonic dependence on T_m in the cylindrical sample chamber while it decreases monotonically in the present sample chamber. It is not clear whether the differences represent dependence of aging on sample size. Smaller sample size would introduce more disorder within the sample and stronger aging effect.

As the sample chamber mounted on the TO oscillates, the chamber walls exert shear stress onto the solid ^{4}He sample which reacts back onto the walls [13,14,42,43]. This back action by the solid ^{4}He sample can change the resonant frequency and the oscillation amplitude of the TO. The back action is dependent on the shear modulus of the solid ^{4}He sample. Temperature dependence and hysteretic response of the shear modulus of solid ^{4}He samples have been observed [5] to be similar to those of the fre-

quency shifts of TO. These similarities suggest some underlying link between the shear modulus and the TO effects though there are reports [44] to the contrary. If the link did exist, aging behavior similar to those reported here would be expected in the shear modulus of solid ^{4}He. To our knowledge, long-relaxation effects have not been reported with shear modulus of solid ^{4}He.

"Condensation"of ^{3}He impurity atoms onto dislocation lines was suggested [5] as the mechanism for immobilizing the dislocation lines and consequently for the observed upturn in shear modulus of solid ^{4}He at low temperatures. If the ^{3}He condensation mechanism is important, it is possible that a time dependent process of ^{3}He impurity atoms condensing onto dislocation lines produces time dependent shear modulus and hence time dependent mechanical coupling to TO. Iwasa [45] argued that the hysteresis [6] observed in TO experiments may be explained by the number of condensed ^{3}He impurity atoms dependent on the sample velocity and temperature. In our protocol of aging experiment, as the drive amplitude is decreased to half of the starting value, condensing ^{3}He atoms provide more pinning points of dislocation lines. The stiffened dislocation lines increases the TO frequency and decreases (increases) the dissipation (TO response amplitude) associated with the line motion. However, it is difficult to understand the observed undershoot with this mechanism.

When the drive amplitude is decreased to half in the measurement protocol, the average acceleration of the sample decreases by a factor of 4. The accompanying small change in average pressure within the sample may not occur instantaneously if dislocation line motions are involved. However, it is again difficult to reconcile the observed undershoot when the pressure change occurs monotonically.

In similar experiments as by Aoki *et al*. [24], Choi *et al*. [46] measured long time TO response after increases in drive amplitude. They found no "overshoot" response in agreement with our [24] earlier work, but they observed a logarithmic time dependence in contrast to ours. It is known [6] that the direction of change in the drive amplitude strongly affects the TO response. Direct comparison between their and present results is not possible since relaxation response changes as the measurement protocol is changed.

It has been argued [12–14] that the observed frequency shift and dissipation peak of TO containing solid ^{4}He could be explained by ascribing a glassy response to a subsystem of dislocation lines with a range of relaxation times. Their analysis has been extended [15] to the measurements frequency and dissipation of our double TO. It would be of great interest to compare the present results with predictions on aging phenomena that follow from their glass description of solid ^{4}He.

Nonequilibrium transient behavior similar to those described in this report is seen in other systems. For example, measurements [47] carried out on a disordered two-dimensional electron system in silicon metal–oxide–semiconductor show that when the applied gate voltage is suddenly decreased the conductivity undergoes a rapid undershoot before recovering slowly towards steady value. Unlike our system, however, collapse of the observed time dependent conductivity [48] when plotted against the ratio t/t_w is similar to the simple aging behavior in spin glasses.

6. Summary

Measurements of the response of a torsional oscillator loaded with disordered solid ^{4}He following reduction in drive amplitude were carried out in analogy to the remanent magnetization of field cooled spin glasses. The reduction in drive amplitude was made after waiting (or aging) time t_w between several minutes and 25 h has elapsed after cooling the sample through an onset transition temperature T_s for "slowing down" to a given measurement temperature. The time t dependent response amplitude showed "undershoots" just after the reduction in drive amplitude, then partially recovered with exponential, and finally logarithmic time dependence. The "undershoots" disappeared above $T_s \sim 40$ mK. The TO responses after various values of waiting time t_w could not be represented by a single function of the reduced time t/t_w. The inflection point times of the response did not vary in proportion to t_w. These two findings clearly showed that disordered solid ^{4}He did not exhibit the glassy behavior similar to those of spin glasses. However, the magnitude of undershoot, the characteristic time of partial recovery magnitude and the rate of logarithmic increase all showed aging effect with logarithmic dependence on t_w. The mechanism for the observed dependence on t_w has not been identified.

We thank Jennifer Yu and Victoria Yu for design and construction of the torsional oscillator reported in this report, David Ruffner, Michael Keiderling and Vaibhav Sharma for assistance in data acquisition, Christian Enss for discussion on glassy behaviors, and especially Gergely Zimányi a conversation motivating our aging experiments.

The research was supported by grants from NSF, DMR-0704120 and DMR-1005325.

Appendix: effect of solid ^{4}He in fill tube

The torsion rod in our TO is an open tube which acts both as a filling passage to the sample chamber and as the torsion member. Solid ^{4}He is formed both in the fill tube and the sample chamber. The solid grown in the fill tube contributes to the effective torsion constant of the torsion rod. If the complex shear modulus of solid ^{4}He in the fill tube changes, the effective torsion constant changes. This will then produce changes in the frequency and amplitude of the TO. It was pointed [36] out that the fill tube effect may be significant in our TO.

Table 1. Comparison of frequency shifts in three double compound torsional oscillators. In each TO, the torsion rod is identical except the sample chamber. For each sample chamber, quantities (measured mode frequencies f_i, loading frequencies Δf_i, frequency shifts δf_i at low temperature, and expected (see text) frequency shifts $\delta f_{i\mu}$ from 30% changes in shear modulus of solid ^{4}He within the torsion rod) are given for the low ($i = 1$) and high ($i = 2$) mode and "ratio" is the high mode value divided by the low mode value of each quantity

Sample chamber	Cylinder [6]			1 mm wide annulus [9]			0.2 mm wide annulus [9,38]		
	$i = 1$	$i = 2$	ratio	$i = 1$	$i = 2$	ratio	$i = 1$	$i = 2$	ratio
f_i, Hz	497	1171	2.4	493	1164	2.4	465	1092	2.3
Δf_i, Hz	0.667	2.05	3.07	0.40	1.20	3.0	0.173	0.313	1.8
δf_i, mHz	0.67	2.05	3.06	0.995	3.36	3.4	1.2	8.1	6.8
$\delta f_i / \Delta f_i$	0.0010	0.0010	1.0	0.0025	0.0028	1.1	0.0069	0.026	3.7
$\delta f_{i\mu}$, mHz	0.62	.47	2.36	0.62	1.46	2.36	0.58	1.37	2.35

Possible effects that solid ^{4}He within the fill tube has on our experiments are examined below in three independent TOs fabricated with three different sample chambers but each reattached to the identical torsion rod system. The measured mode frequencies, loading frequencies, frequency shifts at low temperatures and estimated frequency shifts expected from the changes in shear modulus of solid contained within the torsion rod are all tabulated for the three sample chambers in Table 1. Observed maximum increase in shear modulus of solid ^{4}He samples grown by blocked capillary method is near 30%. Expected shift in the ith mode frequency from this change in shear modulus of solid ^{4}He within the torsion rod (assuming the two rods in our double compound TO are identical) is estimated by $\delta f_{i\mu_8} = 0.3(1/2) f_i(\mu_4/\mu_{\mathrm{BeCu}})(r_4/r_{\mathrm{BeCu}})^4$, where $\mu_4 \sim 1.8\cdot 10^8$ is the shear modulus of solid ^{4}He, $\mu_{\mathrm{BeCu}} = 5.8\cdot 10^{11}$ the shear modulus of the BeCu rod, r_4 the radius of fill tube and r_{BeCu} the radius of the BeCu rod (numerical values given in CGS units).

As it can be seen in Table 1, the measured δf_i in the case of cylindrical sample chamber is indeed quite close to $\delta f_{i\mu}$. Note, however, that the ratio $\delta f_2/\delta f_1$ is significantly larger than $\delta f_{2\mu}/\delta f_{1\mu}$ ($= f_2/f_1$). The measured frequency dependence of δf_i does not match that of the shear modulus effect. In the annular sample chambers, the measured δf_i is larger than the calculated $\delta f_{i\mu}$ by a factor between 1.5 and 6 depending on the mode. Furthermore, the frequency dependence of the shift as indicated by the ratio $\delta f_2/\delta f_1$ is much greater than that of the ratio $\delta f_{2\mu}/\delta f_{1\mu}$ calculated from the maximum 30% expected change in shear modulus. From these clear discrepancies between δf_i and $\delta f_{i\mu}$, it is concluded that the major portions of observed frequency shifts, as well as response amplitudes, in our TO result from the interaction between the ^{4}He sample and its chamber not the torsion rod.

The ratio $\delta f_i/\Delta f_i$ represents NCRI fraction as it has been called in the literature. If this fraction is to be interpreted as superfluid fraction, it is expected to be independent of frequency. Table 1 shows that $\delta f_i/\Delta f_i$ is independent of the mode frequency in the cylindrical chamber but it becomes increasingly more dependent on frequency in thinner annular channels. Barring extremely strong size dependence on restricted geometry, this frequency dependence is contrary to interpreting NCRIf as a superfluid fraction. The observed dependence on the width of the annular chamber is not in proportion to the square of the annulus width as predicted [43] by considering the elastic influence of solid ^{4}He on TO.

1. E. Kim and M. Chan, *Nature (London)* **427**, 225 (2004).
2. E. Kim and M. Chan, *Science* **305**, 1941 (2004).
3. D.E. Galli and L. Reatto, *J. Phys. Soc. Jpn*. **77**, 1010 (2008).
4. S. Balibar and F. Caupin, *J. Phys. Condens. Matter* **20**, 173201 (2008).
5. J. Day and J. Beamish, *Nature (London)* **450**, 853 (2007).
6. Y. Aoki, J.C. Graves, and H. Kojima, *Phys. Rev. Lett*. **99**, 015301 (2007).
7. E. Kim, J.S. Xia, J.T. West, X. Lin, A.C. Clark, and M.H.W. Chan, *Phys. Rev. Lett.* **100**, 065301 (2008).
8. R. Toda, P. Gumann, K. Kosaka, M. Kanemoto, W. Onoe, and Y. Sasaki, *Phys. Rev. B* **81**, 214515 (2010).
9. P. Gumann, M.C. Keiderling, D. Ruffner, and H. Kojima, *Phys. Rev. B* **83**, 224519 (2011).
10. D.Y. Kim and M.H.W. Chan, *Phys. Rev. Lett*. **109**, 155301 (2012).
11. G. Biroli, C. Chamon, and F. Zamponi, *Phys. Rev. B* **78**, 224306 (2008).
12. A.V. Balatsky, M.J. Graf, Z. Nussinov, and S.A. Trugman, *Phys. Rev. B* **75**, 94201 (2007).
13. Z. Nussinov, A.V. Balatsky, M.J. Graf, and S.A. Trugman, *Phys. Rev. B* **76**, 014530 (2007).
14. M. Graf, Z. Nussinov, and A. Balatsky, *J. Low Temp. Phys*. **158**, 550 (2010).
15. M. Graf, J.-J. Su, H. Dahal, I. Grigorenko, and Z. Nussinov, *J. Low Temp. Phys*. **162**, 500 (2011).
16. M. Boninsegni, N. Prokof'ev, and B. Svistunov, *Phys. Rev. Lett*. **96**, 105301 (2006).
17. S. Gaudio, E. Cappelluti, G. Rastelli, and L. Pietronero, *Phys. Rev. Lett*. **101**, 075301 (2008).
18. A.F. Andreev, *JETP Lett*. **85**, 585 (2007).
19. A.F. Andreev, *JETP* **109**, 103 (2009).
20. A. Andreev, *J. Low Temp. Phys*. **168**, 126 (2012).
21. S.E. Korshunov, *JETP Lett*. **90**, 156 (2009).

22. D.C. Vural and A.J. Leggett, *J. Non-Cryst. Solids* **357**, 3528 (2011).
23. A.S.C. Rittner and J.D. Reppy, *Phys. Rev. Lett*. **98**, 175302 (2007).
24. Y. Aoki, M.C. Keiderling, and H. Kojima, *Phys. Rev. Lett*. **100**, 215303 (2008).
25. B. Hunt, E. Pratt, V. Gadagkar, M. Yamashita, A.V. Balatsky, and J.C. Davis, *Science* **324**, 632 (2009).
26. E.J. Pratt, B. Hunt, V. Gadagkar, M. Yamashita, M.J. Graf, A.V. Balatsky, and J.C. Davis, *Science* **332**, 821 (2011).
27. E.C. Heltemes and C.A. Swenson, *Phys. Rev*. **128**, 1512 (1962).
28. D. Edwards and R. Pandorf, *Phys. Rev. A* **140**, 816 (1965).
29. X. Lin, A.C. Clark, Z.G. Cheng, and M.H.W. Chan, *Phys. Rev. Lett*. **102**, 125302 (2009).
30. V.N. Grigor'ev, V.A. Maidanov, V.Y. Rubanskii, S.P. Rubets, E.Y. Rudavskii, A.S. Rybalko, Y.V. Syrnikov, and V.A. Tikhii, *Phys. Rev. B* **76**, 224524 (2007).
31. P. Granberg, L. Sandlund, P. Nordblad, P. Svedlindh, and L. Lundgren, *Phys. Rev. B* **38**, 7097 (1988).
32. E. Vincent, J.P. Bouchaud, D.S. Dean, and J. Hammann, *Phys. Rev. B* **52**, 1050 (1995).
33. E. Bouchaud, *J. Phys. Condens. Matter* **9**, 4319 (1997).
34. B. Bakó, I. Groma, G. Gyrgyi, and G.T. Zimányi, *Phys. Rev. Lett*. **98**, 075701 (2007).
35. Y. Aoki, J. Graves, and H. Kojima, *J. Low Temp. Phys*. **150**, 252 (2008).
36. J.R. Beamish, A.D. Fefferman, A. Haziot, X. Rojas, and S. Balibar, *Phys. Rev. B* **85**, 180501 (2012).
37. A. Leggett, *Phys. Rev. Lett*. **25**, 1543 (1970).
38. P. Gumann, M. Keiderling, and H. Kojima, *J. Low Temp. Phys*. **168**, 162 (2012).
39. Y. Aoki and H. Kojima, *Unpublished* (2008).
40. L. Lundgren, P. Svedlindh, P. Nordblad, and O. Beckman, *Phys. Rev. Lett*. **51**, 911 (1983).
41. E. Vincent, J. Hammann, M. Ocio, J.-P. Bouchaud, and L.F. Cugliandolo, *Slow Dynamics and Aging in Spin Glasses*, in: *Lect. Notes Phys*. E. Rubi (ed.) Berlin Springer Verlag (1997), Vol. 492, p. 184. arXiv:cond-mat/9607224.
42. H.J. Maris, *Phys. Rev. B* **86**, 020502 (2012).
43. J. Reppy, X. Mi, A. Justin, and E. Mueller, *J. Low Temp. Phys*. **168**, 175 (2012).
44. H. Choi, D. Takahashi, K. Kono, and E. Kim, *Science* **330**, 1512 (2010).
45. I. Iwasa, *J. Low Temp. Phys*. **171**, 30 (2013).
46. H. Choi, S. Kwon, D.Y. Kim, and E. Kim, *Nat. Phys.* **6**, 424 (2010).
47. J. Jaroszyński and D. Popović, *Phys. Rev. Lett*. **96**, 037403 (2006).
48. J. Jaroszyński and D. Popović, *Phys. Rev. Lett*. **99**, 046405 (2007).